The Astrophysical Journal, 832:86 (5pp), 2016 November 20 doi:10.3847/0004-637X/832/1/86

SN2002es-LIKE SUPERNOVAE FROM DIFFERENT VIEWING ANGLES

Yi Cao[1], S. R. Kulkarni[1], Avishay Gal-Yam[2], S. Papadogiannakis[3], P. E. Nugent[4,5], Frank J. Masci[6], and Brian D. Bue[7]
[1] Astronomy Department, California Institute of Technology, Pasadena, CA 91125, USA
[2] Department of Particle Physics and Astrophysics, Weizmann Institute of Science, Rehovot 76100, Israel
[3] The Oskar Klein Centre, Department of Physics, Stockholm University, SE-106 91 Stockholm, Sweden
[4] Department of Astronomy, University of California, Berkeley, CA 94720-3411, USA
[5] Lawrence Berkeley National Laboratory, 1 Cyclotron Road, MS 50B-4206, Berkeley, CA 94720, USA
[6] Infrared Processing and Analysis Center, California Institute of Technology, Pasadena, CA 91125, USA
[7] Jet Propulsion Laboratory, California Institute of Technology, Pasadena, CA 91125, USA
Received 2016 June 17; revised 2016 September 11; accepted 2016 September 12; published 2016 November 18

ABSTRACT

In this article, we compare optical light curves of two SN2002es-like Type Ia supernovae (SNe), iPTF14atg and iPTF14dpk, from the intermediate Palomar Transient Factory. Although the two light curves resemble each other around and after maximum, they show distinct early-phase rise behavior in the *r*-band. On the one hand, iPTF14atg revealed a slow and steady rise that lasted for 22 days with a mean rise rate of 0.2–0.3 mag day^{-1}, before it reached the *R*-band peak (-18.05 mag). On the other hand, iPTF14dpk rose rapidly to -17 mag within a day of discovery with a rise rate >1.8 mag day^{-1}, and then rose slowly to its peak (-18.19 mag) with a rise rate similar to iPTF14atg. The apparent total rise time of iPTF14dpk is therefore only 16 days. We show that emission from iPTF14atg before -17 days with respect to its maximum can be entirely attributed to radiation produced by collision between the SN and its companion star. Such emission is absent from iPTF14dpk probably because of an unfavored viewing angle, provided that SN2002es-like events arise from the same progenitor channel. We further show that an SN2002es-like SN may experience a dark phase after the explosion but before its radioactively powered light curve becomes visible. This dark phase may be lit by radiation from supernova–companion interaction.

Key words: supernovae: general – supernovae: individual (SN2002es, iPTF14atg, iPTF14dpk)

1. INTRODUCTION

Type Ia supernovae (SNe Ia) are explosions of carbon–oxygen white dwarfs (WDs). There are two leading scenarios about their origins. In the single-degenerate (SD) channel, WDs accrete mass from non-degenerate companion stars and explode when their masses approach the Chandrasekhar mass limit. In the double-degenerate channel, merging or collision of WD pairs in binary or triple systems triggers the SN explosions (see Maoz et al. 2014 for a recent review).

There are multiple subclasses of SNe Ia in observations: Branch normal, SN1991T, super-Chandrasekhar, SN1991bg, Iax, SN2002es, etc. The Type Iax (Foley et al. 2013) and SN2002es-like (Ganeshalingam et al. 2012) subclasses have low expansion velocities. Type Iax SNe lack Ti II absorption lines in their spectra and favor young stellar populations, whereas SN2002es-like events show prominent Ti II troughs and are associated with old stellar population (White et al. 2015). Both low-velocity SNe are possibly pure deflagration of WDs. Their low expansion velocities and large amount of intermediate-mass elements are consistent with incomplete subsonic burning of carbon and oxygen (e.g., Fink et al. 2014). Recent observations appear to find direct evidence for companion stars of two Type Iax SNe (Foley et al. 2014; McCully et al. 2014) and an SN2002es-like SN (Cao et al. 2015).

Following the discovery of a strong and declining UV pulse from an SN2002es-like supernova iPTF14atg within four days of explosion (Cao et al. 2015), it becomes particularly interesting to examine the early-phase light curve of other SN2002es-like events. If the UV pulse in iPTF14atg indeed arises from collision between the SN-ejected material and a companion star, then due to the effect of viewing angle it should be invisible in most other SN2002es-like events.

Thanks to nightly cadence surveys conducted as part of the intermediate Palomar Transient Factory (iPTF; Law et al. 2009; Rau et al. 2009; Cao et al. 2016), we found two SN2002es-like events between 2013 and 2015, internally designated as iPTF14atg and iPTF14dpk. Both events have well-sampled optical light curves and spectroscopic coverage. In this article, we compare the early-phase rise behaviors of these two events.

The article is organized as follows. In Section 2 we establish their similarities to SN2002es. In Section 3 we compare the different rise behaviors of the two events and seek an explanation. We conclude in Section 4.

2. SIMILARITY OF THE TWO EVENTS

Observations of iPTF14atg and iPTF14dpk were undertaken in the Mould *R* filter with the 48 inch Schmidt telescope at Palomar Observatory. Their light curves are produced by the PTF-IPAC forced photometry pipeline (Masci et al. 2016) which uses pre-SN reference images to subtract the host galaxy light, and performs point-spread function photometry at the location of a transient on the difference images. All magnitudes in this paper are in the AB system and calibrated to the PTF-IPAC catalog (Ofek et al. 2012b).

The spectra of iPTF14atg were published in Cao et al. (2015). The spectra of iPTF14dpk were obtained at -10 days with respect to its peak with the double spectrograph (Oke & Gunn 1982) on the Palomar 200 inch Hale telescope, and at $+20$ and $+50$ days with the Low Resolution Imaging Spectrometer (Oke et al. 1995) on the Keck-I telescope at Mauna Kea. The spectra were reduced using standard IRAF/

Table 1
Two SN2002es-like Events in iPTF

Name	Coordinates (J2000)	Redshift	μ[a]	Host Type	$E(B-V)$[b]	Peak MJD[c]	Peak Mag.[c]
iPTF14atg	$12^h52^m44^s.84$ $+26°28'13''.0$	0.0213	34.92	E-S0	0.011	56802.1	-18.05 ± 0.02
iPTF14dpk	$16^h45^m19^s.35$ $+40°09'41''.3$	0.0387	36.23	Starburst	0.012	56878.1	-18.19 ± 0.02

Notes.
[a] The distance moduli μ are calculated with $H = 67.77$ km s^{-1} Mpc^{-1} (Planck Collaboration et al. 2014). No redshift-independent distance measurement is available for the host galaxies of these events on the NASA/IPAC Extragalactic Database (NED).
[b] The map of Galactic extinction is given by Schlafly & Finkbeiner (2011).
[c] The peak modified Julian dates (MJD) and magnitudes are measured from the PTF R-band light curves. The peak magnitudes do not include uncertainties from μ.

IDL routines. The spectra are made public through WISeREP (Yaron & Gal-Yam 2012).

In order to correct for the Galactic extinction, we use the model of Fitzpatrick (1999), assuming $R_V = 3.1$. Regarding the host galaxy extinction, since the equivalent widths of Na I D absorption lines are correlated with the local extinction (Poznanski et al. 2012), the absence of Na I D absorption at the redshifts of the host galaxies in the spectra suggests that neither iPTF14atg nor iPTF14dpk is embedded in a dusty circumstellar medium. In fact, using the spectra of iPTF14atg and iPTF14dpk with highest signal-to-noise ratios, and assuming that the width of the Na I D doublet is 200 km s^{-1}, we derived 3σ upper limits on the equivalent width of the doublet: <0.20 Å for iPTF14atg and <0.75 Å for iPTF14dpk. According to the empirical relation in Poznanski et al. (2012), these upper limits on the equivalent width correspond to $E(B-V) < 0.02$ and $E(B-V) < 0.11$, respectively. In the following analysis, we do not correct for local extinction.

The primary data from the two events are summarized in Table 1. Their light curves and spectra are shown in Figures 1 and 2, respectively.

Next, in order to determine their peak magnitudes and dates, we use Gaussian process regression to interpolate the light curves (Figure 1). A squared exponential function is chosen as the autocorrelation function and the autocorrelation length is determined by the maximum likelihood estimation based on available data. Thanks to the almost nightly photometric sampling, the regression analysis determines both the peak dates and magnitudes with small uncertainties, as shown in Table 1.

We calculate k-correction in the Mould R-band for these two SNe using their spectra. We find that the k-correction is $\lesssim$0.2 mag at their redshifts. Hence, we neglect the k-correction from here onward.

As shown in Figure 1, apart from the first few days after explosions, the light curves of both iPTF14atg and iPTF14dpk are quite similar. Since the Mould R filter is similar to the SDSS r filter (Ofek et al. 2012a), light curves of both iPTF14atg and iPTF14dpk also resemble the r-band light curve of SN2002es around maximum, though iPTF14atg does not show the fast decline seen in SN2002es after $t \simeq 30$ days. The peak magnitudes of iPTF14atg ($R = -18.05$ mag), iPTF14dpk ($R = -18.19$ mag), and SN2002es ($r = -18.35$ mag) are also comparable within the slight filter difference.

As can be seen in Figure 2, the spectra of iPTF14atg and iPTF14dpk around and after maxima also match those of SN2002es at similar phases. In particular, both iPTF14atg and iPTF14dpk show the low-velocity absorption lines and Ti II troughs, the hallmark of SN2002es-like SNe. Next, the spectra of iPTF14atg and iPTF14dpk taken at -10 days share broad

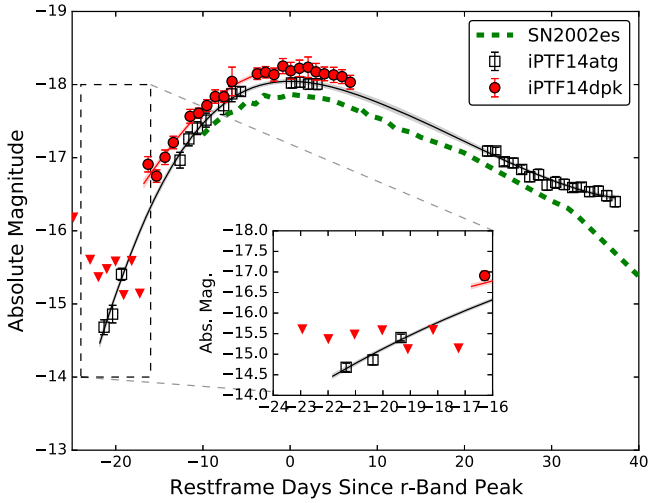

Figure 1. Light curves of iPTF14atg and iPTF14dpk. Black empty squares are iPTF14atg and red filled stars denote iPTF14dpk. Detection upper limits (5σ) of pre-SN non-detections for iPTF14atg and iPTF14dpk are denoted by black empty and red filled downward triangles, respectively. The best interpolated light curves of iPTF14atg and iPTF14dpk with uncertainties from the Gaussian process regression are shown as red and black curves, respectively. For comparison, the green dashed curve shows the r-band light curve of SN2002es. The inset zooms in on the early-phase light curves of iPTF14atg and iPTF14dpk for better illustration.

absorption features, although the continuum emission of iPTF14dpk appears bluer than that of iPTF14atg. This color difference might be due to residuals from imperfect subtraction of galaxy light in the spectra of iPTF14dpk, because iPTF14dpk is located close to the center of its apparently blue and compact host galaxy in an interacting galaxy pair. Therefore, we do not think that the blueness of iPTF14atg indicates a significant difference from iPTF14dpk.

Integrating the spectra and calibrating to the broadband photometry, we obtain an optical luminosity of 3×10^{42} erg s^{-1} for both SNe around maximum. Since SN radiation around maximum is concentrated in the optical, the optical luminosity is a good approximation to the bolometric luminosity. In the case of iPTF14atg, the date of explosion is tightly constrained by the SN–companion collision, and therefore its rise time to the R-band maximum is 22 days. The total ^{56}Ni mass can be estimated from the peak luminosity and the rise time via the following equation (Arnett 1982):

$$L_{\rm max} = \alpha S(t_R), \quad (1)$$

where $S(t_R)$ is the instantaneous radioactive power at the peak of the light curve. Under the assumption that the heating

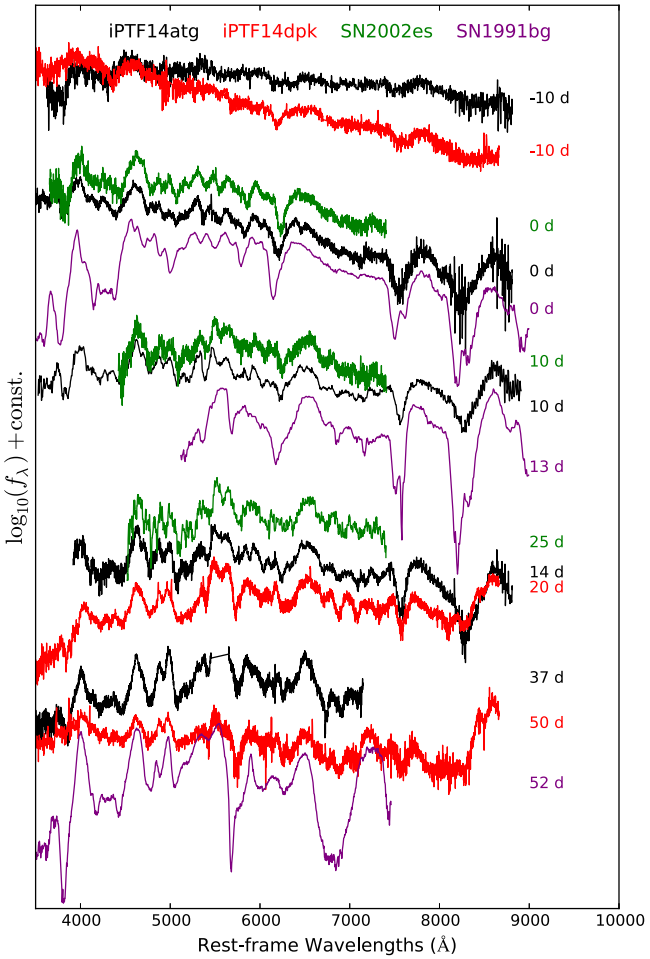

Figure 2. Spectral sequences of iPTF14atg and iPTF14dpk. The iPTF14atg spectra are taken from Cao et al. (2015) and shown in black while the iPTF14dpk spectra are in red. For comparison, we also show spectra of SN2002es (green; Ganeshalingam et al. 2012) and SN1991bg (purple, Filippenko et al. 1992). The phase of each spectrum is shown next to the spectrum.

timescale is much shorter than the evolution timescale of the SN, $S(t)$ can be expressed as

$$\frac{S(t)}{10^{43}\ \mathrm{erg\ s^{-1}}} = [6.31\exp(-t/8.8) + 1.43\exp(-t/111)]\frac{M_{\mathrm{Ni}}}{M_{\odot}}, \quad (2)$$

where t is in units of days. α is an efficiency factor of order unity, depending on the distribution of ^{56}Ni. We adopt a fiducial value of $\alpha = 1.3$ here following Scalzo et al. (2012). Then we estimate a total ^{56}Ni mass of 0.14 $M_{\odot}$ for iPTF14atg.

In contrast, as discussed in Section 3, iPTF14dpk may experience a "dark" period after the explosion. Therefore its light curve only provides an upper limit on the actual date of explosion, or equivalently a lower limit on the rise time, and thus a lower limit of 0.11 $M_{\odot}$ on the ^{56}Ni mass.

In addition, we would like to clarify that the main difference of SN2002es-like events from "classical" subluminous SN1991bg-like events is that the former exhibit low-velocity absorption features. As shown in Figure 2, around maximum, although the overall spectral shapes look similar among SN2002es-like events and SN1991bg, the velocities of the absorption lines, such as Si II, are obviously lower in SN2002es-like events than in SN1991bg by several thousand km s^{-1}. At late times, SN2002es-like events develop multiple narrow features between 5000 and 7000 Å, while these features are blended in the spectra of SN1991bg-like events (Jha et al. 2006).

3. LIGHT CURVES AT EARLY PHASES

As noted in the previous section, iPTF14atg and iPTF14dpk exhibit different photometric behaviors at early phases. In particular, iPTF14atg took more than a week to rise to -17 mag with a mean rise rate of 0.2–0.3 mag day^{-1}. In contrast, iPTF14dpk shows a steep rise to $r = -16.9$ mag within one day of its last non-detection of $r > -15.1$ mag, indicating an initial rise rate >1.8 mag day^{-1}. In the subsequent epoch, the apparent decline in the light curve of iPTF14dpk is not statistically significant.

At first sight, the pre-discovery 5σ upper limits of iPTF14dpk in the magnitude plot may mislead readers into concluding that the upper limits of iPTF14dpk are roughly consistent with the early detections of iPTF14atg. However, the last upper limit of iPTF14dpk is below the interpolated light curve of iPTF14atg by more than half a magnitude. Furthermore, if iPTF14dpk had had the same light curve as iPTF14atg, then stacking the last four pre-discovery images of iPTF14dpk would result in a detection well above 5σ. The non-detection in the stacked image reiterates that iPTF14dpk has a different initial rise from iPTF14atg.

3.1. SN–companion Interaction

Next, we seek an explanation for the distinct early-phase light curves of the two otherwise similar SNe. Given the spectroscopic typing and almost identical light curves (apart from the early rise), we make a simple and reasonable assumption that *all* SN2002es-like events arise from the same progenitor channel. As noted in Cao et al. (2015), the observed early declining UV pulse from iPTF14atg provides evidence for the SD progenitor channel.

Three energy sources may power the optical light curve of an SN from the SD channel: SN shock breakout, SN–companion collision, and radioactive decay of ^{56}Ni. The shock breakout of an SN Ia lasts for less than a second (Piro et al. 2010), so we do not consider this energy resource to explain the light curves of iPTF14atg and iPTF14dpk.

Both the component powered by SN–companion collision and the component powered radioactively are seen in the light curve of iPTF14atg. Specifically, its UV/optical light curve before -17 days is dominated by the Rayleigh–Jeans tail of the signature of the SN–companion interaction, and the light curve after -17 days is mainly from radioactive decay. In order to show this, we fit the SN–companion collision model (Kasen 2010) to its early UV light curve, Noting that a factor of π is missing in the calculation of Cao et al. (2015), we find a good fit with an explosion energy of 3×10^{50} erg, an ejecta mass of 1.4 $M_{\odot}$, and a binary separation of 70 $R_{\odot}$. Then we calculate the R-band light curve from this model and compare it to the observed R-band light curve. As shown in the upper panel of Figure 3, the light curve before -17 days can be entirely attributed to the Rayleigh–Jeans tail emission from the SN–companion collision. In later epochs, radiation from the

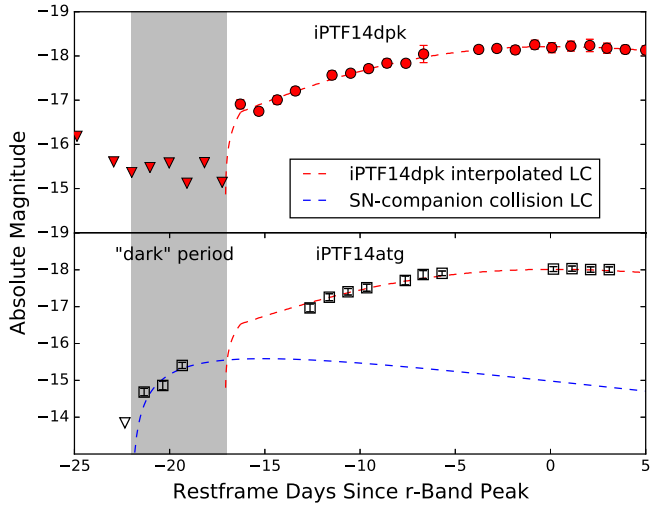

Figure 3. The upper and lower panels show the early *R*-band light curves of iPTF14dpk (red circles) and iPTF14atg (black squares), respectively. In the upper panel, the red dashed curve shows the interpolated light curve of iPTF14dpk from the Gaussian process regression (Section 2). In order to show the initial sharp rise, a power-law curve is used to smoothly extrapolate the light curve up to the pre-discovery upper limit. In the lower panel, the interpolated light curve of iPTF14dpk (red dashed curve) is used as a template light curve and is offset by 0.2 mag to match the observed light curve of iPTF14dpk after −17 days. The blue dashed curve is calculated from the SN–companion collision model to interpolate the emission of iPTF14atg before −17 days (Kasen 2010; Cao et al. 2015). In both panels, the "dark" phases are highlighted in gray.

SN–companion interaction becomes minor and the light curve has to be powered by the radioactive energy.

In fact, as noted by Kasen (2010), given typical mass ratios of a few for SD progenitor binaries of SNe Ia, fewer than 10% of the resulting explosions would have a geometry that would allow the signature of the SN–companion collision to be seen by a randomly located observer. For the remaining >90% of events, we can see only the radioactively powered light curves. This provides a natural explanation for iPTF14dpk: its observed light curve is powered purely by its radioactive decay.

If we make a further assumption that iPTF14atg and iPTF14dpk have similar ejecta structures, then their radioactively powered light curves have similar shapes. Despite the observed 0.1 mag difference at peak magnitudes, which is probably due to the exact amount of synthesized ^{56}Ni, the light curve of iPTF14atg can be roughly treated as a superposition of the light curve of the SN–companion collision and that of iPTF14dpk (Figure 3).

3.1.1. A Side Note about iPTF14dpk

The sharp rise of iPTF14dpk was initially considered to be a possible signature of an SN–companion interaction, but our further analysis soon rejected this hypothesis. According to the scaling relations in Kasen (2010), the luminosity from an SN–companion collision is $L \propto aE^{7/8}M^{-7/8}$ and the effective temperature $T \propto a^{-1/4}$, where a is the binary separation, E is the explosion energy, and M is the total ejecta mass. Since the temperature is very high, the radiative flux in the *r*-band can be approximated by the Rayleigh–Jeans law, i.e., $f_\nu \simeq L/(\sigma T^4) \times 2kT\nu^2/c^2 \propto LT^{-3} \propto E^{7/8}M^{-5/8}a^{1/4}$. Hence, the *R*-band flux is insensitive to the binary separation. If iPTF14dpk has an ejecta mass similar to iPTF14atg, then in order to fit the first detection of $r = -17$ mag of iPTF14dpk, its explosion energy has to be $E \gtrapprox 2 \times 10^{51}$ erg. Such a large explosion energy would then lead to an expansion velocity significantly higher than the low expansion velocity of iPTF14dpk derived from its spectral lines. Furthermore, as the effective temperature remains high, the expansion of the SN would make the *R*-band flux increase rapidly with time. However, we do not see a fast-rising light curve after the first epoch of iPTF14dpk.

3.2. SN Dark Phase

Given a binary separation of 70 $R_\odot$ and an ejecta velocity of 5×10^3 km s^{-1}, the SN ejecta of iPTF14atg hit its companion star within three hours of the SN explosion. Here the signature of the SN–companion interaction provides an accurate approximation to the exact time of explosion for iPTF14atg, i.e., at −22.1 days. Given the similarity between iPTF14atg and iPTF14dpk, it is reasonable to assume that the rise time of iPTF14dpk is similar to that of iPTF14atg. In this framework we explore the physical consequences below.

As shown in the lower panel of Figure 3, the radioactively powered light curve of iPTF14dpk was not visible until −16 days. This soon leads to an interesting inference that iPTF14dpk had a "dark" period between its explosion and the first light of its radioactively powered light curve. In our framework, this "dark" period also existed in iPTF14atg, but was illuminated by the signature of the SN–companion interaction. If iPTF14atg had been observed from a different viewing angle, then the signature of the SN–companion interaction would become invisible and hence the "dark" period would appear.

The "dark" period is essentially the time lag before the ^{56}Ni atoms that synthesized during the SN explosion are really able to heat up the photosphere. Qualitatively, a highly mixed ^{56}Ni distribution will quickly heat the photosphere and make the SN visible. In contrast, if ^{56}Ni atoms are confined in the very center of the ejecta, then it will take a while for the energy released from radioactive decay to diffuse past the photosphere and become visible to us.

A "dark" phase has also been suggested in the normal Type Ia SN2011fe (Hachinger et al. 2013; Piro & Nakar 2014). Very recently, Piro & Morozova (2016) calculated light curves of SNe with various distributions of 0.5 $M_\odot$ ^{56}Ni in a 1.25 $M_\odot$ WD model. They found that low ^{56}Ni mixing may lead to a "dark" period of a couple of days after explosion.

In comparison, the estimated "dark" period of about five days in iPTF14dpk seems quite long. Such a long "dark" period might be because iPTF14dpk produces only ∼0.1 $M_\odot$ ^{56}Ni, much less than a normal SN Ia, and because the synthesized ^{56}Ni is buried deeply inside the ejecta material of mass close to the Chandrasekhar limit. Future observations of a very nearby SN2002es-like event will be useful to estimate the total ejecta mass and the distribution of ^{56}Ni.

Our estimate of the length of the "dark" period depends on how the two light curves of iPTF14dpk and iPTF14atg are aligned. Currently the dates of maximum light, which are derived from the best-bit interpolated light curves from the Gaussian process regression, are used. We caution that the actual peak of the light curve may differ by a couple of days, which in turn adds an uncertainty of a couple days to the length of the "dark" period. This uncertainty may be minimized once a template light curve of SN2002es-like SNe is built by future observations.

4. DISCUSSION AND CONCLUSION

In this article, we present optical observations of two low-velocity SNe Ia, iPTF14atg and iPTF14dpk, from the iPTF. Both are photometrically and spectroscopically similar to the prototypical SN2002es (Ganeshalingam et al. 2012). Despite their similarities around and after maximum, we observed different initial rise behaviors in these two events. While iPTF14atg experiences a steady and slow rise that lasts for 22 days, iPTF14dpk shows a sharp initial rise to -16.9 mag within a day of discovery and then joins the rise behavior of iPTF14atg. The apparent rise time of iPTF14dpk is only 16 days.

Based on the spectroscopic typing and similar photometric evolution, and based on the observed early declining ultraviolet pulse in iPTF14atg (Cao et al. 2015), we make a reasonable assumption that all SN2002es-like events arise from the single-degenerate progenitor channel. By analyzing the early *R*-band light curves of iPTF14atg and iPTF14dpk, we show that:

1. The light curve of iPTF14atg can be decomposed into a component from the early SN–companion interaction and the late radioactively powered component. The latter component resembles the full light curve of iPTF14dpk. The absence of the early component in iPTF14dpk is due to an unfavored viewing angle from which the SN–companion interaction is blocked by the optically thick ejecta in the line of sight.
2. An SN2002es-like event, or for that matter any SN Ia in general (Hachinger et al. 2013; Piro & Nakar 2014), may experience a "dark" phase between the actual explosion and the first light of its radioactively powered light curve. The duration of the "dark" phase is the timescale for the radioactive decay energy to reach the SN photosphere.
3. In the case of iPTF14atg, the "dark" phase was illuminated by Rayleigh–Jeans emission from the SN–companion collision.

In future, the collection of a large sample of young SN2002es-like light curves will be valuable in verifying the effect of viewing geometry as well as the "dark" periods. This sample will also put constraints on the geometry of the progenitor binaries for SN2002es-like events and thus the mass ratio. For example, if the mass ratio between the donor and the primary WD is one, then we would have to find 14 young SN2002es-like events before we could observe the SN–companion interaction again.

The upcoming Zwicky Transient Facility (ZTF; Smith et al. 2014) and the planned wide-field fast-cadence ultraviolet surveys, such as ULTRASAT (Sagiv et al. 2014), will provide opportunities to collect the sample in the optical and ultraviolet, respectively. Assuming that the rate of SN2002es-like events is about 10% of the normal rate of SNe Ia, we estimate that ZTF will discover eight young SN2002es-like events every year and that ULTRASAT will find a dozen in its two-year mission lifetime. These two projects, together with other ongoing and planned fast-cadence surveys, will provide a big sample from which to estimate the observational occurrence of the SN–companion interaction and therefore to put constraints on the geometry of the progenitor binaries. Additionally, since the presence of a companion star in an SN explosion adds asphericity to the SN ejecta, spectropolarimetric follow-up observations of SN2002es-like supernovae will also provide independent constraints on the viewing angles (Kasen et al. 2004).

Y.C. and P.E.N. acknowledge support from the DOE under grant DE-AC02-05CH11231, Analytical Modeling for Extreme-Scale Computing Environments. Y.C. also acknowledges support by the GROWTH project funded by the National Science Foundation under Grant No 1545949. A.G.-Y. is supported by the EU/FP7 via ERC grant no. 307260, the Quantum Universe I-Core programme by the Israeli Committee for Planning and Budgeting and the ISF; by Minerva and ISF grants; by the Weizmann-UK "making connections" programme; and by Kimmel and ARCHES awards.

This research used resources of the National Energy Research Scientific Computing Center, a DOE Office of Science User Facility supported by the Office of Science of the U.S. Department of Energy under Contract No. DE-AC02-05CH11231. Part of this research was carried out at the Jet Propulsion Laboratory, California Institute of Technology, under a contract with the National Aeronautics and Space Administration.

REFERENCES

Arnett, W. D. 1982, ApJ, 253, 785
Cao, Y., Kulkarni, S. R., Howell, D. A., et al. 2015, Natur, 521, 328
Cao, Y., Nugent, P. E., Kasliwal, M. M., et al. 2016, PASP, 128, 114502
Filippenko, A. V., Richmond, M. W., Branch, D., et al. 1992, AJ, 104, 1543
Fink, M., Kromer, M., Seitenzahl, I. R., et al. 2014, MNRAS, 438, 1762
Fitzpatrick, E. L. 1999, PASP, 111, 63
Foley, R. J., Challis, P. J., Chornock, R., et al. 2013, ApJ, 767, 57
Foley, R. J., McCully, C., Jha, S. W., et al. 2014, ApJ, 792, 29
Ganeshalingam, M., Li, W., Filippenko, A. V., et al. 2012, ApJ, 751, 142
Hachinger, S., Mazzali, P. A., Sullivan, M., et al. 2013, MNRAS, 429, 2228
Jha, S., Branch, D., Chornock, R., et al. 2006, AJ, 132, 189
Kasen, D. 2010, ApJ, 708, 1025
Kasen, D., Nugent, P., Thomas, R. C., & Wang, L. 2004, ApJ, 610, 876
Law, N. M., Kulkarni, S. R., Dekany, R. G., et al. 2009, PASP, 121, 1395
Maoz, D., Mannucci, F., & Nelemans, G. 2014, ARA&A, 52, 107
Masci, F. J., et al. 2016, PASP, submitted
McCully, C., Jha, S. W., Foley, R. J., et al. 2014, Natur, 512, 54
Ofek, E. O., Laher, R., Law, N., et al. 2012a, PASP, 124, 62
Ofek, E. O., Laher, R., Surace, J., et al. 2012b, PASP, 124, 854
Oke, J. B., Cohen, J. G., Carr, M., et al. 1995, PASP, 107, 375
Oke, J. B., & Gunn, J. E. 1982, PASP, 94, 586
Piro, A. L., Chang, P., & Weinberg, N. N. 2010, ApJ, 708, 598
Piro, A. L., & Morozova, V. S. 2016, ApJ, 826, 96
Piro, A. L., & Nakar, E. 2014, ApJ, 784, 85
Planck Collaboration, Ade, P. A. R., Aghanim, N., et al. 2014, A&A, 571, A16
Poznanski, D., Prochaska, J. X., & Bloom, J. S. 2012, MNRAS, 426, 1465
Rau, A., Kulkarni, S. R., Law, N. M., et al. 2009, PASP, 121, 1334
Sagiv, I., Gal-Yam, A., Ofek, E. O., et al. 2014, AJ, 147, 79
Scalzo, R., Aldering, G., Antilogus, P., et al. 2012, ApJ, 757, 12
Schlafly, E. F., & Finkbeiner, D. P. 2011, ApJ, 737, 103
Smith, R. M., Dekany, R. G., Bebek, C., et al. 2014, Proc. SPIE, 9147, 79
White, C. J., Kasliwal, M. M., Nugent, P. E., et al. 2015, ApJ, 799, 52
Yaron, O., & Gal-Yam, A. 2012, PASP, 124, 668